



ELSEVIER

Available online at [www.sciencedirect.com](http://www.sciencedirect.com)

ScienceDirect

journal homepage: [www.elsevier.com/locate/he](http://www.elsevier.com/locate/he)

# Cell level modeling of the hygrothermal characteristics of open cathode polymer electrolyte membrane fuel cells

Mehdi Andisheh-Tadbir<sup>a</sup>, Andrew Desouza<sup>b</sup>, Majid Bahrami<sup>a</sup>, Erik Kjeang<sup>a,\*</sup>

<sup>a</sup> School of Mechatronic Systems Engineering, Simon Fraser University, 250-13450 102 Avenue, Surrey, BC V3T 0A3, Canada

<sup>b</sup> Ballard Power Systems, Inc., 9000 Glenlyon Parkway, Burnaby, BC V5J 5J8, Canada

## ARTICLE INFO

### Article history:

Received 25 January 2014

Accepted 11 July 2014

Available online 5 August 2014

### Keywords:

Fuel cell

Open cathode

Air-cooled

Hygrothermal

Temperature

Relative humidity

## ABSTRACT

Open cathode designs that utilize ambient air for both cooling and oxygen supply are a useful feature for low- to medium-power polymer electrolyte membrane fuel cell (PEMFC) stacks. Elimination of balance-of-plant subsystems greatly reduces the complexity, parasitic power, and cost of the overall system, and therefore increases the appeal of open cathodes. The present research addresses the key challenges of open-cathode PEMFCs related to thermal management and membrane hydration, two highly coupled phenomena. Accurate knowledge of the temperature and relative humidity (RH) distributions in the cell is essential in order to optimize heat removal by suitable strategies. In the present work, a three-dimensional numerical model is developed that can predict the hygrothermal characteristics in a complete open-cathode cell. The model is validated using experimental data obtained with Ballard Power Systems' FCgen<sup>®</sup>-1020ACS stack under a range of operating conditions. The model is then used to analyze the key flow conditions and properties that control the hygrothermal behavior of open-cathode stacks. Based on the obtained results, flow conditions can affect temperature and RH distributions significantly; in-plane plate thermal conductivity can provide a uniform temperature distribution while adversely reducing the RH; and edge cooling can increase temperature and RH gradients in the cell. Recommendations for hygrothermal design and operation of open cathode stacks are provided.

Copyright © 2014, Hydrogen Energy Publications, LLC. Published by Elsevier Ltd. All rights reserved.

## Introduction

Fuel cells are considered as the “21st century energy-conversion devices for mobile, stationary, and portable

power” [1]. An open cathode fuel cell that utilizes natural or forced convection of ambient air as the main oxygen supply is an emerging type of polymer electrolyte membrane fuel cell (PEMFC) technology which has certain advantages and challenges when compared to the more commonly employed

\* Corresponding author.

E-mail address: [ekjeang@sfu.ca](mailto:ekjeang@sfu.ca) (E. Kjeang).  
<http://dx.doi.org/10.1016/j.ijhydene.2014.07.049>

0360-3199/Copyright © 2014, Hydrogen Energy Publications, LLC. Published by Elsevier Ltd. All rights reserved.

humidified and liquid-cooled PEMFC. The open cathode fuel cell type is simple in terms of system design and maintenance, but complex in terms of hygrothermal management. Elimination of balance of plant subsystems such as liquid coolant loop and gas humidifier reduces the system complexity and cost which is important for commercialization. Ballard Power Systems, as one of the leading fuel cell companies in the world, recognized the importance of open-cathode PEMFCs and pioneered the product development in this area. As a result, an open cathode air-cooled PEMFC stack is currently manufactured by Ballard with the FCgen<sup>®</sup>-1020ACS product designation (cf., Fig. 1(a)). This stack can operate in various ambient conditions and the output power is scalable from 300 W to 3 kW.

In order to unlock the far-reaching potential of PEMFC technology, a wide variety of research and development activities are currently underway in both industry and academia. Major advances in this field often rely on modeling to guide experimental and development work. Common modeling approaches in fuel cell science and technology were recently reviewed by Wang [1]. Fuel cell modeling is a complex process, because it deals with multi-scale geometries, electrochemical reactions, mass and heat transfer, and deformation phenomena. A comprehensive fuel cell model should include the transport equations from the nano- and micro-scale catalyst layers, gas diffusion layers, and membrane to mini-scale channels and large-scale stacks with multiple cells with consideration of solid, ionomer, gas, and liquid phases. However, considering the available computational resources, it is not possible to include all the details in such models. Hence, depending upon the fuel cell conditions, the required accuracy, and the aim of the research, different modeling scenarios may emerge. Many research activities to date considered macroscopic modeling [2–7] while others focused on pore scale modeling of different fuel cell components [8–10]. The recent trends in macroscopic fuel cell modeling of relevance for open-cathode designs were directed towards thermal management, flow field design, and water management. The issues related to the water and thermal management are particularly important when dealing with the open cathode air-cooled PEMFCs. This is attributed to the low humidity operating conditions and limited cooling effectiveness. Most established fuel cell models assume fully hydrated membranes and isothermal conditions [11–13] which are

generally acceptable for liquid-cooled fuel cells operating under well-humidified conditions. However, such assumptions are not valid for open cathode designs, known to operate under low humidity conditions and have significant temperature gradients [14].

Thermal management is a necessity for PEMFCs, especially for the air-cooled stacks. Heat generation inside the cells and its distribution could result in different thermal behavior of the stack. Ju et al. [15] examined different heat generation mechanisms in a single channel PEMFC. Their model was accurate in predicting the thermal behavior on the single-channel level; however, it could not capture the temperature or RH gradients on the cell level. Bapat and Thynell [16] studied the effects of anisotropic thermal properties and contact resistance on the temperature distribution using a two-dimensional single-phase model based on a single channel domain, but did not investigate the effects of those properties on the RH distribution. Several useful thermal management strategies have been developed for PEMFCs. Installation of separate liquid cooling channels in the bipolar plate is the most common strategy to avoid high temperatures. This approach was experimentally examined by Matian et al. [17]. Wider cooling channels were shown to enhance the rate of heat transfer from the stack with the tradeoffs of reduced mechanical stability and increased complexity of plate design and manufacturing. The Ballard Nexa stack pioneered the use of air cooling through a separate flow field configuration [18]. However, due to their complexity, the Nexa stack was replaced with the modern Ballard FCgen<sup>®</sup>-1020ACS stack with combined cathode air supply and cooling channels. Alternative strategies are also available in the literature that may increase the complexity of the stack design and operation under transient conditions [19,20].

Another important phenomenon in low humidity air-cooled stacks is membrane dehydration. Membrane water content, which is a function of water activity, will directly affect proton conductivity [12] and consequently ohmic losses. It is shown in Ref. [21] that low humidity operation will reduce the overall fuel cell performance. Therefore, self-humidifying MEAs should be utilized to avoid membrane dehydration. A vast amount of research is focused on water transport modeling and water management in PEMFCs. These investigations are mostly directed towards resolving the flooding issues under high humidity conditions [22,23] in

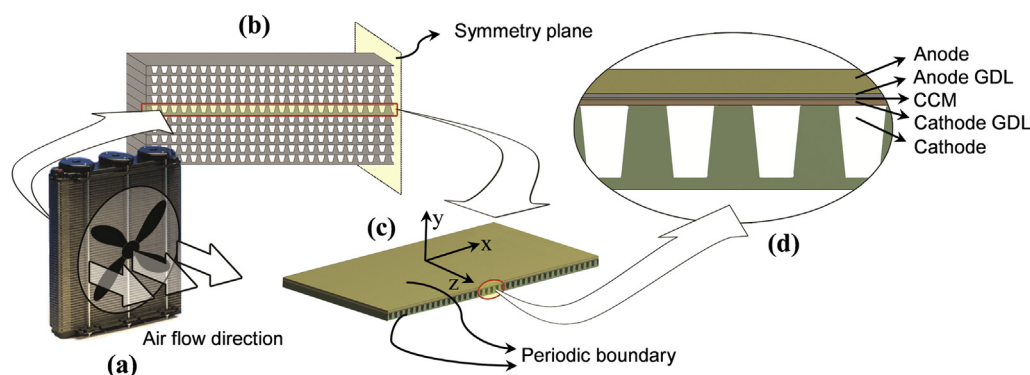


Fig. 1 – Model geometry, cell components, and boundary conditions.

order to increase power density. In air-cooled fuel cells, however, drying is more critical than flooding. Zhang et al. [24] compared the fuel cell performance obtained experimentally with fully humidified and completely dry gases under isothermal conditions, and found that the cell performance decreased at dry conditions due to poor ionomer phase proton conductivity. It was also demonstrated that cell operation at a combination of dry gases and high temperature was particularly challenging. No such studies have been reported for open cathode and/or air-cooled PEMFCs, known to operate under dry, non-isothermal conditions [14].

Temperature and membrane hydration are highly coupled during fuel cell operation and pose significant challenges for open-cathode stacks that lack the homogenous characteristics of standard, liquid cooled and humidified PEMFCs. By proper hygrothermal management of PEMFCs, the operating temperature of the stack as well as the membrane hydration level ought to be controlled in the desired range, i.e., between 60 and 100 °C for temperature [25] and higher than 15–20% for RH. Even though a host of studies were carried out on PEMFC modeling, no work is reported in the literature on the investigation of stack hygrothermal characteristics. Simultaneous study of heat and humidity can provide the fuel cell manufacturers with precious information. Such information can be utilized in designing a system that will not face the aforementioned problems. Our group recently developed a computational thermal model for the central cathode channel in an air-cooled PEMFC system [14]. This model could reasonably predict the maximum temperature in the air-cooled stack. However, it was limited to the analysis of a single cathode channel, not a complete cell.

To investigate the hygrothermal characteristics of open-cathode air-cooled stacks and assess their behavior under various conditions, a specialized cell-level numerical model is developed in this work. The model includes one complete fuel cell situated in an air-cooled stack and can predict the temperature and humidity distribution inside the cell efficiently and accurately. The present model is validated with experimental data obtained at Ballard Power Systems, and applied to locate hot spots and dry zones throughout the whole cell. In addition, an investigation on stack hygrothermal characteristics is performed by considering the effects of the flow rate, flow distribution, in-plane plate thermal conductivity, and edge cooling. Finally, practical recommendations are made for passive hygrothermal control of the stack, which could enhance fuel cell performance and durability without increasing cost.

## Modeling approach

The main objective of this work is to develop a model that can predict the hygrothermal characteristics in a cell of an open-cathode PEMFC stack. Therefore, the temperature and humidity distributions inside the cell are the key parameters of interest. The present modeling scheme is based in part on the thermal model developed previously by our group [14]; however, in this work the model is extended to solve for humidity in order to capture the hygrothermal coupling. Moreover, since the computational domain is extended to a complete cell

instead of a single channel, more useful studies can be performed to investigate the effects of different parameters on the hygrothermal characteristics of the stack, especially in the cell lateral-direction. The geometry and governing equations of the present model are described in the following subsections.

## Model geometry

The left part of Fig. 1 shows a schematic of the Ballard FCgen<sup>®</sup>-1020ACS which is an open cathode air-cooled scalable PEMFC stack. This stack consists of a variable number of cells that are stacked vertically. The cathode channels used jointly for oxygen supply and cooling are straight and the air is provided by a fan placed near the outlet. On the anode side, the channels are dead-ended and filled by stagnant pressurized hydrogen. The hydrogen channels are purged periodically during operation. In this analysis, one cell of a generalized open cathode stack is modeled and the governing equations for its heat and mass transfer are solved numerically in three dimensions. The geometrical model and boundary conditions are depicted in Fig. 1. Periodic boundary conditions are applied at the top and bottom sides of the plate, which is representative of a given cell in the main body of the stack. Note that the symmetric boundary is invalid in this case due to the lack of symmetry in the x-z plane and heat transfer between adjacent cells. For the inlet and outlet boundaries, constant pressure is set, and the inlet air composition based on the ambient relative humidity and temperature is defined. The cell shown in Fig. 1(b) has a symmetry boundary condition at the central symmetry plane on the right and a convection heat transfer boundary condition at the edge of the cell on the left. The positions of the main MEA components including the catalyst coated membrane (CCM) and GDLs that are considered in this model are shown in Fig. 1(d).

## Governing equations

The physics of the model are governed by the conservation of mass, momentum, chemical species, and energy. Since the channel Reynolds number is less than 2300, even for the highest volumetric flow rate considered here, laminar flow is assumed. In addition, the flow is incompressible as a result of low Mach numbers inside the channels.

The general form of the mass conservation equation for an incompressible steady state flow is shown in Eq. (1), in which  $\rho$  is the gas mixture density,  $\vec{V}$  is the velocity, and  $S_{\text{mass}}$  is the mass source term for the electrochemical reactions in the cell:

$$\nabla \cdot (\rho \vec{V}) = S_{\text{mass}} \quad (1)$$

$$S_{\text{mass}} = -\frac{M_{\text{O}_2} J}{4F} + \frac{M_{\text{H}_2\text{O}} J}{2F} \quad (2)$$

In Eq. (2),  $M$  is the molar mass,  $F$  is the Faraday's constant, and  $J$  is the volumetric current density. Here,  $J$ , which is equal to the current density divided by the CCM thickness, is assumed to be known *a priori* based on the measured current density distributions. More details about this assumption are explained in Section 3.

Conservation of momentum is brought in Eq. (3), where  $p$  is the gas pressure and  $\mu$  is the mixture viscosity that can be obtained from the mass-weighted mixing law theory shown in Eq. (4):

$$\nabla \cdot \rho \vec{V} \vec{V} = -\nabla p + \nabla \cdot (\mu \nabla \cdot \vec{V}) + S_{\text{Mom}} \quad (3)$$

$$\mu = \sum_i \frac{\chi_i \mu_i}{\sum_j \chi_j \phi_{ij}}, \quad i, j = \text{O}_2, \text{N}_2, \text{H}_2\text{O} \quad (4)$$

In Eq. (4),  $\chi_i$  is the mole fraction of each chemical species and  $\phi_{ij}$  has the following formulation:

$$\phi_{ij} = \frac{\left[ 1 + \left( \frac{\mu_i}{\mu_j} \right)^{1/2} \left( \frac{M_j}{M_i} \right)^{1/4} \right]^2}{\left[ 8 \left( 1 + \frac{M_i}{M_j} \right) \right]^{1/2}} \quad (5)$$

The last term in the momentum equation is the source term which is only non-zero in the porous GDL and CCM layers. In other words, a sink is added to the general momentum equation that represents the flow resistance due to the existence of porous materials. This source term can be obtained from the following equation:

$$S_{\text{Mom}} = -\frac{\mu}{\kappa} \vec{V} \quad (6)$$

where  $\kappa$  is the gas permeability inside a porous medium.

Conservation of energy and chemical species equations are shown in Eqs. (7) and (8), respectively:

$$\nabla \cdot (c_p \rho \vec{V} T) = \nabla \cdot (k \nabla T) + S_T \quad (7)$$

$$\nabla \cdot (\rho \vec{V} Y_j) = \nabla \cdot (\rho D_{\text{eff}} \nabla Y_j) + S_j \quad j = \text{O}_2, \text{N}_2, \text{H}_2\text{O} \quad (8)$$

where  $c_p$  is the specific heat of the mixture calculated from Eq. (9) and  $k$  is the mixture thermal conductivity obtained based on the weighing model used for the viscosity (cf., Eq. (4)).  $Y_j$  is the mass fraction of the  $j$ th species in the mixture and  $D_{\text{eff}}$  is the effective diffusion coefficient, assumed to be constant.

$$c_p = \sum_i Y_i c_{p,i} \quad (9)$$

The last terms in Eqs. (7) and (8) are the source terms. In Eq. (7), the source term is the total heat generation rate which consists of reversible and irreversible heat losses calculated from Eq. (10) [26]. Similarly in Eq. (8), the source term represents consumption of oxygen and production of water vapor obtained from Eq. (11):

$$S_T = (E_{\text{th}} - V_{\text{cell}}) J \quad (10)$$

$$S_{\text{O}_2} = -\frac{J}{4F} M_{\text{O}_2}, \quad S_{\text{H}_2\text{O}} = \frac{J}{2F} M_{\text{H}_2\text{O}} \quad (11)$$

In Eq. (10),  $E_{\text{th}}$  is the thermal voltage [24] defined by Eq. (12) and  $V_{\text{cell}}$  is the cell voltage. The cell voltage and current density distribution are applied based on measured data.

$$E_{\text{th}} = \frac{-\Delta H}{2F} \quad (12)$$

Here, the low heating value of hydrogen,  $\Delta H$ , is used to calculate the thermal voltage, i.e., the product water is

assumed to be generated in the vapor phase. Furthermore, since the stack operates at low humidity conditions, high air flow rates, and relatively low current densities, it is expected that there will be no water vapor condensation. In contrast to most previous cell/stack level simulations, see for example [27], a uniform current density assumption is not required in the present model, which is essential for accurate modeling of open cathode devices with large gradients. Here, the coupled heat and mass transfer equations are solved simultaneously and the distribution of heat and water vapor generation is assumed to be a function of the current density distribution.

Commercial software, ANSYS Fluent 14.0, is used to solve the governing equations. The SIMPLE algorithm is implemented to solve the pressure–velocity coupling and the power-law scheme is used for the discretization of the equations. A mesh independency study is performed for different mesh sizes, and finally a structured mesh with 3.1 million cells is chosen. For the convergence criterion of  $1.0 \times 10^{-6}$  for the absolute error, the solution converges after 250 iterations. This number will increase to 500 if  $1.0 \times 10^{-12}$  is chosen for the convergence criterion. Approximately 4–6 h are required for 500 iterations in parallel mode with 4 cores on an Intel® Core™ i7 Processor system with 12 GB RAM.

## Results and discussion

The unique cell-level hygrothermal model of an open cathode air-cooled fuel cell developed in this work is first validated with experimental data measured using a standard stack configuration and then applied to investigate the key hygrothermal characteristics of the stack under a range of typical operating conditions.

### Model validation

Fig. 2 shows the normalized current density distribution measured at different locations in a single cell within a Ballard Power Systems FCgen®-1020ACS stack. The normalization is performed based on the average cell current density.

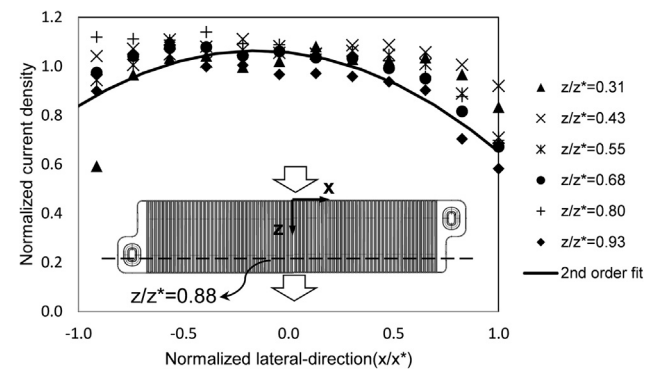


**Fig. 2 – Normalized current density distribution measured at different downstream positions (indicated by the symbols) along the lateral direction (indicated by the dashed line) of a single cell in the center of the stack.**



Experimental observations show that the normalized current density distribution is essentially independent of the stack power rating. Therefore, it is possible to use the same normalized distribution for different stack power levels. This assumption is valid as long as no major changes are made in the stack geometry. Moreover, as inferred from Fig. 2, the variations of current density along the downstream position,  $z/z^*$ , are small. Hence, it is assumed that the current density is only a function of the lateral position, i.e., the distribution is one dimensional.

To examine the validity of these two assumptions, two different scenarios are considered. In the first one, the simulated temperatures by using 1D and 2D current density distributions are compared to the measured temperature data. Fig. 3 shows the temperature distribution along the lateral direction in the cell at the downstream position of  $z/z^* = 0.88$  for the first scenario. The difference between implementation of 1D and 2D distribution is less than 2.8%. Hence, variations of current density along the channel direction can be neglected.

In the second scenario, simulated and measured temperatures for two typical stack power levels are compared at  $z/z^* = 0.88$ . Since the 1D current density distribution provides reasonable accuracy, the same assumption is used here. Details on the stack operating conditions for the two power levels are tabulated in Table 1. Demonstrated in Fig. 4 are the obtained results for this scenario. Good agreement can be seen between the model predictions and the experimental measurements. As shown in Fig. 4 for  $x/x^* > 0$ , which indicates the right half of the cell, the deviation between the present numerical model and the experimental data is larger. This is due to the assumption of symmetric boundary condition at the center. The FCgen<sup>®</sup>-1020ACS stack does not have completely symmetric cells and the current density distribution, as a consequence of the non-uniform temperature distribution, is not fully symmetric (cf., Fig. 2). In general, the numerical results from the model are in good agreement with

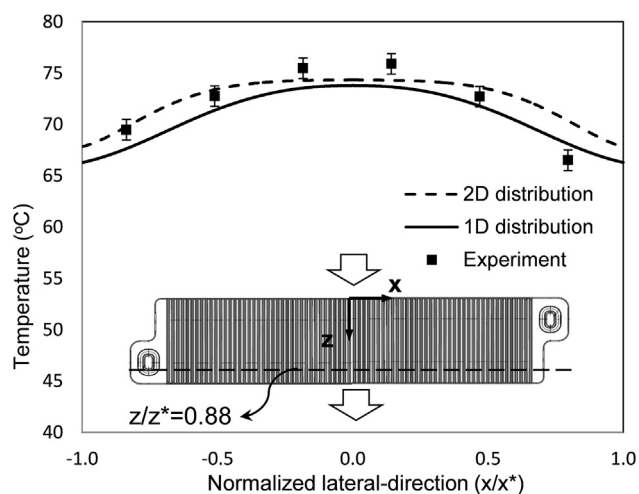


**Fig. 3 – Temperature distribution at  $z/z^* = 0.88$ . Square symbols represent experimental data; solid line indicates modeling results with 2D current distribution assumption; and dashed line shows modeling results with 1D current distribution assumption.**

**Table 1 – Operating conditions of the stack used for model validation.**

|                          | Case A | Case B |
|--------------------------|--------|--------|
| Stack current (A)        | 87.0   | 57.1   |
| Cell voltage (V)         | 0.569  | 0.712  |
| Air flow rate (lpm)      | 86.7   | 29.6   |
| Ambient temperature (°C) | 21     | 20     |

the experimental data and the maximum relative difference is less than 6%.

### Case studies

In this section, the validated cell-level model is applied to simulate and assess the variations of hygrothermal stack characteristics under a practical range of conditions and cell parameters. Firstly, a number of case studies are performed to investigate the effect of key parameters on the temperature and RH distributions in the cell. Then, based on the obtained results, recommendations are made to improve the hygrothermal management of the cell/stack by increasing temperature and RH uniformity throughout the cell and mitigating local hot spots and dry zones. The cathode air flow rate, the overall fan velocity distribution at the cathode outlet, the bipolar plate thermal conductivity, and different edge cooling scenarios are the main influential parameters expected to control the hygrothermal characteristics of the cell. As such, the above-mentioned cases are investigated to provide useful guidelines for improved design and operation of open cathode air-cooled PEMFCs.

### Baseline case

An open cathode cell with the dimensions and operating conditions listed in Table 2 is considered as the baseline case. The conditions assumed for the baseline case represent a fuel cell with an efficiency of 50% and power output of 110 W per cell. The simulated temperature contours for this case are shown in Fig. 5(a). The maximum temperature is predicted to occur at the outlet of the central channel and the temperature

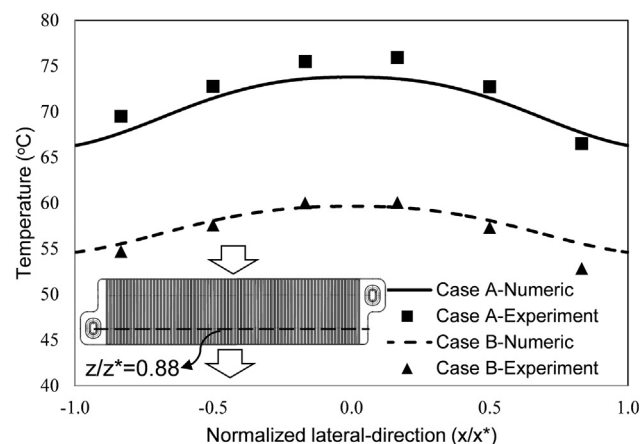


**Fig. 4 – Temperature distribution at  $z/z^* = 0.88$  for two stack power levels obtained by the present model (lines) and from the measurements (symbols).**

gradients in the cell have the same trends as the experimental data. The maximum temperature for this case is calculated to be 79.5 °C.

The simulated RH contours at the interface between the cathode GDL and CCM for the baseline case are presented in Fig. 5(b). In contrast to typical liquid-cooled PEMFCs with gas humidification, air-cooled PEMFCs operate under remarkably dry conditions. Provided that ambient air supply of low temperature and humidity is utilized directly on the cathode, the average RH value in the cathode side of the air-cooled stack is much lower than those of other types of PEMFCs. This can be seen in Fig. 5(b), where the RH is ranging from 10% to 35% for the baseline conditions. The RH is higher under the lands, where the water vapor transport from the MEA to the channel is more constrained than directly under the channel. Moreover, although the water generation rate is higher close to the center of the cell, the RH is lower at those locations. This shows the high dependence of RH on temperature, thus demonstrating the important hygrothermal coupling of the open cathode design. The driest portion of the cell coincides with the highest temperature, which indicates that excessive heat generation can overshadow water production in terms of the overall hygrothermal performance of the cell.

#### Flow distribution

The velocity distribution downstream of a fan is generally not uniform. As a consequence, the flow rate in each channel may vary across the cell, which could affect the hygrothermal characteristics. A preliminary numerical simulation is performed to model the flow inside a stack consisting of 28 plates with 80 channels and baseline dimensions. For this case, only the flow field is solved. Fig. 6 shows the geometric model and the simulation results for a quarter of the aforementioned stack when the fan is placed in suction mode at the cathode outlet. Due to the inherent symmetry of the fan and stack combination, only a quarter of the physical 3D domain is required for fluid dynamics simulations. The obtained velocity profiles at the outlet position of the central cell in the stack for two different fan positions, i.e., 2 cm and 5 cm from the stack, are shown in Fig. 7. The velocity is lower in front of the fan hub and increases toward the blade tips. This is also in agreement with the experiments done in Ref. [28]. In general, the velocity distribution becomes more uniform with increased spacing between fan and stack.

Based on the profile obtained from the experiments in Ref. [28] and the numerical results obtained in this work, a hypothetical velocity profile using a cosine function is proposed at the outlet of the stack:

$$V = V_0 \left[ \left( 1 - \cos\left(\frac{\pi x}{x^*}\right) \right) + \alpha \right] / (2 + \alpha) \quad (13)$$

where  $V_0$  represents the amplitude of the velocity profile and  $\alpha$  is an index that represents the flow uniformity. A high flow uniformity index indicates a more uniform flow.

The proposed velocity distribution is used as the boundary condition for the velocities at the outlet of the cathode channels in the cell level model to assess its impact on the hygrothermal performance of the stack. Fig. 8(a) and (b) present the temperature and RH profiles, respectively, along the lateral direction in the cell at the downstream position of  $z/z^* = 0.8$  for different flow uniformity indices. By decreasing the flow uniformity, i.e., decreasing  $\alpha$ , the temperature and RH gradients in the cell are found to increase significantly. With non-uniform flow, larger areas may be dried out, which can result in lower fuel cell performance.

Although the flow distribution in this work is hypothetical, results from this section reveal the importance of flow uniformity and its impact on the hygrothermal characteristics of air-cooled PEMFCs. Hence, care should be exercised when a fan is selected for cooling purposes in open-cathode stacks. Providing uniform flow to the stack is shown to result in improved hygrothermal characteristics and consequently features increased performance. Moreover, there is an opportunity to control the temperature and RH in the stack by designing suitable manifolds.

#### Fan flow rate

The air flow rate produced by the fan is also an important factor for hygrothermal management of open-cathode fuel cell stacks. As shown by our previous channel-level model [14], the air flow rate reduces the maximum temperature considerably. Using the present cell-level model, a parametric study is performed to examine the effect of air flow rate on the maximum and minimum temperature and RH values in the whole cell. Note that in all cases, a uniform flow distribution is assumed. Shown in Fig. 9 is the variation of the cell maximum and minimum temperature and RH for different air flow rates. By doubling the air flow rate from 50 to 100 lpm, while keeping all other parameters constant at the baseline values, the maximum temperature drops about 25 °C. The maximum temperature differential in the cell is also reduced by 10 °C. 100 lpm for the aforementioned cell dimensions may be considered an artificially high flow rate in the context of conventional, liquid-cooled PEMFCs, but is a typical value used to increase the cooling capacity for air-cooled stacks operating at high current densities.

Both water vapor concentration and temperature increase along the channel due to heat and mass generation inside the CCM and the transport of heat and mass from the inlet towards the outlet. In all cases, the maximum temperature occurs at the outlet near the center of the cell, and its minimum value is found close to the inlet at the corner adjacent to the cell edge (Fig. 5(a)). The same trend is found for the water vapor concentration. However, the case is not the same for

**Table 2 – Baseline case conditions.**

| Parameter                  | Value    |
|----------------------------|----------|
| Stack current              | 80 A     |
| Cell voltage               | 0.57 V   |
| Air flow rate              | 51.5 lpm |
| Ambient temperature        | 20 °C    |
| MEA thickness              | 500 μm   |
| Cathode channel height     | 3.0 mm   |
| Anode thickness            | 1.0 mm   |
| Rib width                  | 1.5 mm   |
| Cathode channel length     | 70.0 mm  |
| Number of cathode channels | 80       |
| Flow distribution          | Uniform  |

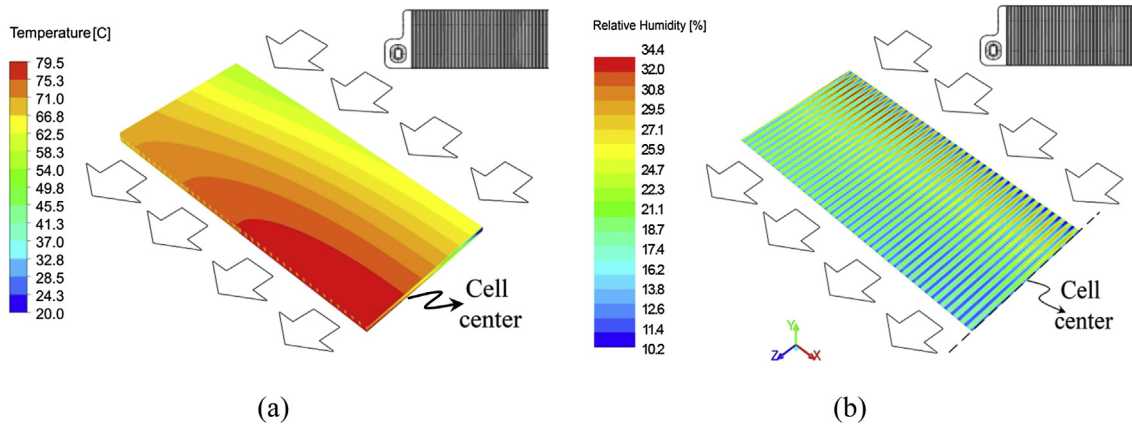


**Fig. 5 – Simulated (a) temperature and (b) RH contours for the baseline open cathode fuel cell. The modeling domain shown here is the left half of a single cell in the stack.**

RH. In contrast to the water vapor concentration, RH is a function of the water saturation pressure which itself is a function of temperature. Therefore, both temperature and water vapor concentration are critical factors in determining RH. The minimum RH in the CCM occurs under the channel at the inlet of the central channel and its maximum is located under the landing at the channel inlet adjacent to the edge of the cell (cf., Fig. 5(b)). The RH variation along the channel direction is found to be monotonically increasing or parabolic, depending on the fuel cell conditions (cf., Fig. 12).

Liquid-cooled, humidified PEMFCs often operate at around 80 °C [29], where an optimum balance is reached between high electrochemical kinetics and adequate membrane hydration. Hence, we may seek a similar operating point for the air-cooled open cathode cells. However, such characteristics are difficult to achieve for operation on ambient air. As shown in Fig. 9, for flow rates below 70 lpm, the minimum RH is equal to or less than 15%, which can be considered an impractically dry condition. Hence, although the air stoichiometry is sufficiently high to provide enough oxygen to the cell, a higher flow rate is required to guarantee adequate hydration.

Temperature and RH have inverse trends according to Fig. 9. As the flow rate increases, both minimum and maximum values of RH increase, while both minimum and

maximum temperatures decrease. Increasing the flow rate thus effectively enhances heat transfer and cools down the system. As a result of the temperature drop, the water saturation pressure is reduced. The water vapor concentration also decreases in the CCM since the mass transfer rate is improved in the channel. Recalling the RH definition,  $RH = \frac{p_v}{p_{sat}} = \frac{x_{H_2O} P}{p_{sat}}$ , both numerator and denominator decrease; however, the net RH increases because of the more rapid decay in saturation pressure.

#### Plate thermal conductivity

Heat conduction through the bipolar plate is one of the major paths of heat transfer in air-cooled stacks. Hence, the thermal conductivity of the plate material is an influential parameter for hygrothermal management. Its importance on thermal management was studied in Ref. [14] for a single channel; however, neither the temperature gradients along the lateral direction nor the humidity distribution were assessed in that model. As an extension to the previous work, in the present work these effects are studied in the whole cell. Fuel cell bipolar plates are usually made of graphite. Graphite is an orthotropic material, which means that its thermal conductivity is direction-dependent with respect to the through-plane and in-plane directions. The in-plane thermal

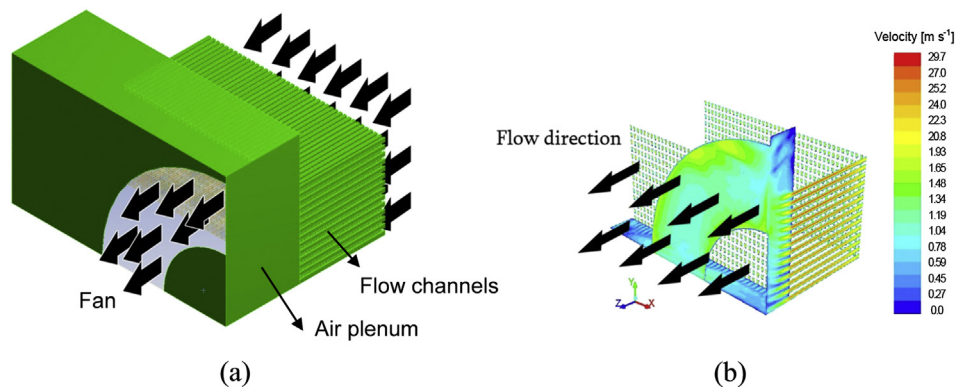


**Fig. 6 – Geometric model for a quarter of the stack used for fluid dynamics simulations, indicating (a) fan, plenum, and flow channel domains and (b) obtained velocity distribution in the stack.**

conductivity of graphite is generally between 10 and 1000 W m<sup>-1</sup> K<sup>-1</sup> [30]. However, its through-plane thermal conductivity is at least 10 to 100 times lower. In this section, the sensitivity of this parameter and its effects on the cell-level hygrothermal characteristics are explored.

Previously in Ref. [14], it was shown that the through-plane thermal conductivity of the bipolar plate, under the considered range, did not have a significant impact on the temperature distribution. Therefore, only the in-plane thermal conductivity is presently examined. It is anticipated that by increasing the thermal conductivity, a more uniform temperature distribution in the cell is achieved. Fig. 10 shows the simulated variations of maximum and minimum temperature and RH in the cell for three different cell currents (20, 60, and 80 A), which correspond to current densities of 0.14, 0.42, and 0.56 A cm<sup>-2</sup>, respectively.

Notably, both temperature and RH in open cathode cells are strong functions of current density. The local temperature in the simulated cell is found to increase from 25 to 30 °C at low cell current to 50–80 °C at high current. By increasing the in-plane thermal conductivity from 60 to 600 W m<sup>-1</sup> K<sup>-1</sup>, the maximum temperature in the plate is found to decrease from 77.7 to 74.5 °C for the baseline case (high current density). This trend is consistent at medium and low current densities despite the lower net operating temperatures. Although the observed drop in maximum temperature is quite small, the maximum temperature difference in the plate, which is a good indicator of temperature gradients in the cell, decreases significantly at all current densities. Therefore, a relatively uniform temperature distribution is obtained. The effect of this parameter on the temperature uniformity is however not significant for values higher than 300 W m<sup>-1</sup> K<sup>-1</sup>, which can be considered a practical target thermal conductivity that is commercially available with emerging materials such as pyrolytic graphite sheets [31].

In contrast to the temperature, the local relative humidity in the simulated cell is determined to decrease significantly from 25 to 70% at low current to 5–35% at high current due to higher heat generation. Hence, open cathode cell operation at high current densities is the most challenging regime and therefore the baseline of this study. At high current, both maximum and minimum values of relative humidity decrease

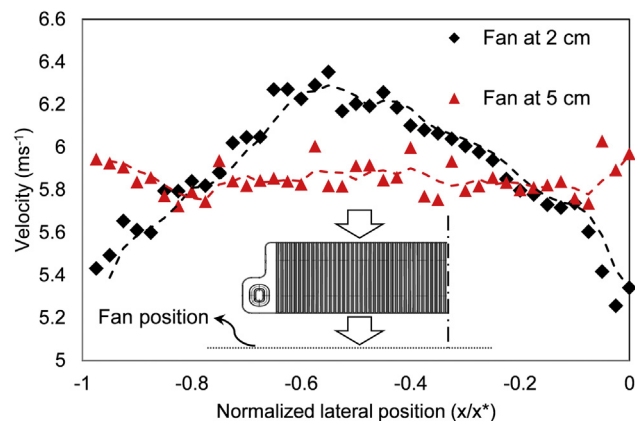


Fig. 7 – Simulated velocity profiles at the outlet of the central cell for two different fan distances from the stack.

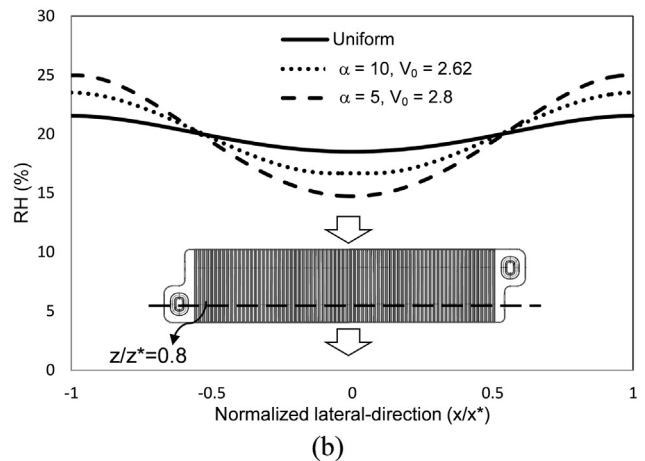
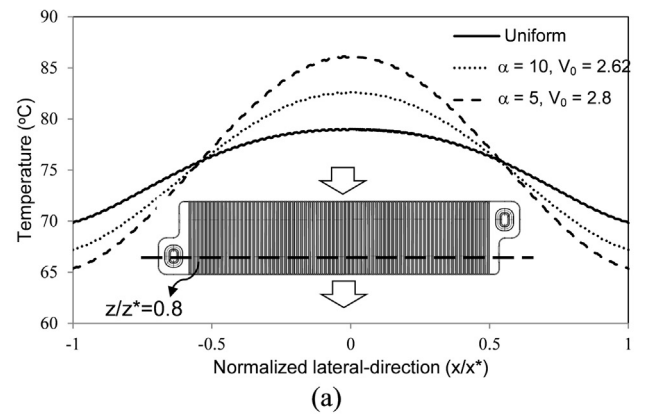


Fig. 8 – Simulated (a) temperature and (b) RH distributions for different flow uniformity indexes,  $\alpha$ , at  $z/z^* = 0.8$ .

as the in-plane thermal conductivity is increased. This is primarily a result of increasing average temperature in the CCM and the strong hygrothermal coupling experienced by open cathode cells. For instance, the average CCM temperature increases by approximately 10 °C when the in-plane thermal conductivity is increased from 60 to 600 W m<sup>-1</sup> K<sup>-1</sup>. The more uniform temperature distribution obtained at higher in-plane thermal conductivities also leads to a more uniform humidity distribution in the cell. This can be seen in Fig. 11, which compares the RH distribution along the lateral direction at two

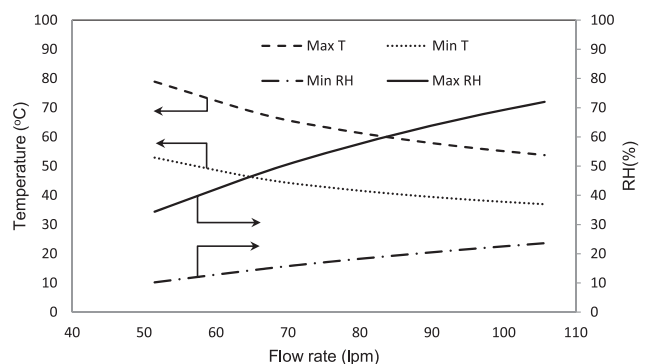
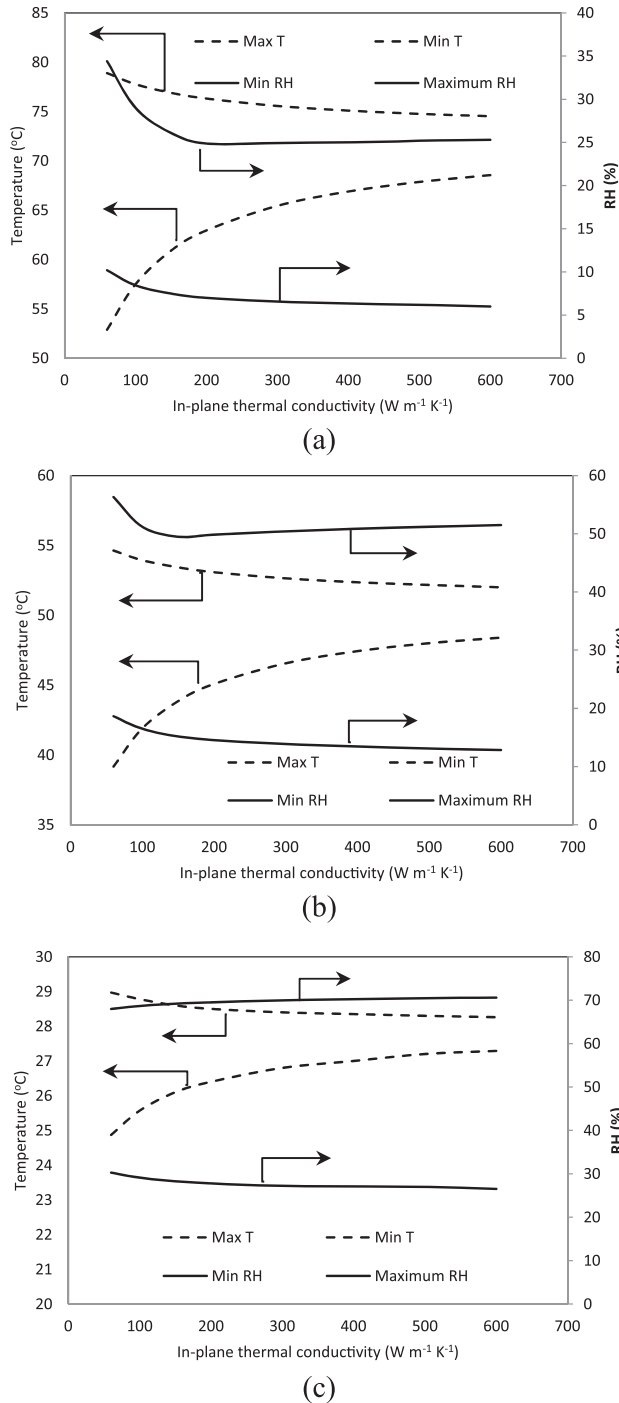


Fig. 9 – Effect of air flow rate on the hygrothermal behavior of an air-cooled open cathode fuel cell stack.



downstream positions, one near the outlet and one near the inlet, for three different plate in-plane thermal conductivity values. It should be mentioned again that similar to the explanation made under Fig. 8(b), for higher clarity of the diagram, the mean RH distribution is shown. The exact RH distribution oscillates around the mean values depending on the lateral position (channel vs. land). A considerable portion of



**Fig. 10** – Effect of plate thermal conductivity on the maximum and minimum temperature and RH in an open cathode cell operating at: (a) high current density, (b) medium current density, and (c) low current density.

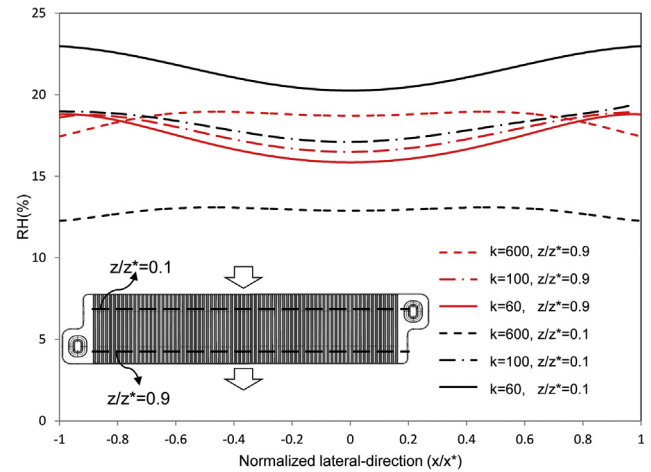


**Fig. 11** – Simulated RH distributions in the cathode catalyst layer at the inlet (black lines) and outlet (red lines) locations for three different in-plane thermal conductivity values (as indicated,  $[\text{W m}^{-1} \text{K}^{-1}]$ ) for the plate. (For interpretation of the references to color in this figure legend, the reader is referred to the web version of this article.)

the distinct difference between the minimum and maximum RH values shown in Fig. 10 is attributed to this oscillation. At the inlet of the cathode channels, the overall RH level is found to decrease with increasing thermal conductivity due to the rise in local temperature. However, at the outlet, the RH values increase as a result of local temperature reduction caused by the enhanced in-plane heat transfer. Note that the enhanced heat transfer attributed to increased in-plane thermal conductivity is influential on RH values both under channels and under lands.

A major finding from Fig. 11 is that the highest thermal conductivity material is not always the best alternative for air-cooled stacks, considering that larger dry zones may emerge by using such materials. As seen in Fig. 11, the moderate in-plane thermal conductivity ( $100 \text{ W m}^{-1} \text{K}^{-1}$ ) leads to more uniform RH distribution along the lateral direction as well as along the channel direction. This trend is further exhibited in

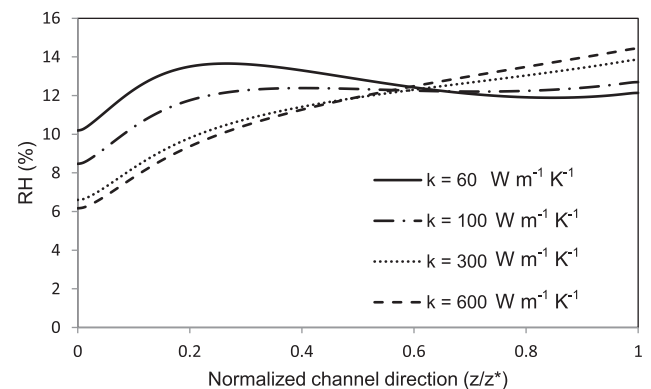


**Fig. 12** – RH variations along the channel direction under the central channel for different plate in-plane thermal conductivities.

Fig. 12 which is brought to assess the variations of RH along the channel direction. Indeed, the moderate in-plane thermal conductivity of  $k = 100 \text{ W m}^{-1} \text{ K}^{-1}$  provides the most uniform RH distribution. Moreover, it is observed that increasing the in-plane thermal conductivity would not affect the RH distribution substantially beyond a critical value, which is  $k = 300 \text{ W m}^{-1} \text{ K}^{-1}$  for the case under consideration. Using high thermal conductivity materials will be beneficial in creating temperature uniformity but results in lower RH values. However, the latter constraint can be mitigated by increasing the flow rate.

#### Edge cooling

The rate of heat transfer from the outer surfaces of the cell to the surrounding environment is another factor that could influence the hygrothermal characteristics of the stack. The convective heat transfer coefficient at these surfaces depends on the natural convection or forced convection regimes for cooling. The simulated temperature and RH profiles at the  $z/z^* = 0.8$  downstream position are presented in Fig. 13 for four different convective heat transfer coefficients at the edge of the cell.

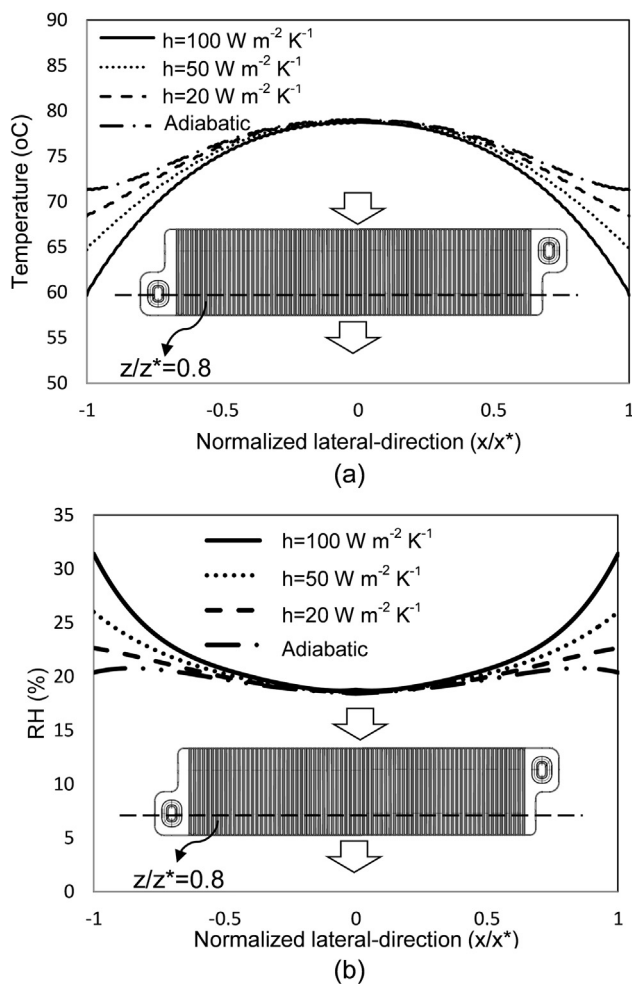


Fig. 13 – (a) Temperature and (b) RH distributions along the lateral direction in the CCM at  $z/z^* = 0.8$  for different edge cooling conditions.

By increasing the heat transfer coefficient at the edges from zero (adiabatic condition) to  $100 \text{ W m}^{-2} \text{ K}^{-1}$  (high speed forced convection), the overall heat removal rate increases which is desirable for high power applications, but the temperature uniformity decreases which is undesirable due to the introduction of thermal stresses in the stack. Furthermore, edge cooling is found to be only effective on the cell areas close to the edges and does not have major effects on the maximum temperature which occurs at the center of the cell.

The RH variation shows the inverse trend of the temperature. According to Fig. 13(b), by increasing the convective heat transfer coefficient, the RH increases due to the drop in the temperature in the regions adjacent to the cell edge. Similarly to the temperature behavior, these changes are limited to the edges and are not effective in the central regions.

It should be noted that the effectiveness of edge cooling depends on the stack width. The theoretical heat dissipation capacity of the edges is simply not sufficient to cool wide stacks such as the ones analyzed in this work due to the relatively high rates of internal heat generation. Small, less wide stacks with merely a few parallel channels may however be effectively cooled through the edges. It is noteworthy however that edge cooling could still have negative effects in such cells due to increased temperature gradients along the lateral direction. A reduced temperature at the edge may also reduce the electrochemical kinetics in that region, the effect of which is beyond the scope of this work. It is also found that the temperature uniformity in case of high convective heat transfer rates can be improved by using a high thermal conductivity material, although temperature gradients are still significant.

## Conclusions

The hygrothermal characteristics of open cathode PEMFC stacks were examined by numerical simulations under various flow and design conditions. A unique cell-level hygrothermal model was developed for this purpose and extensively validated with experimental data. Significant coupling of temperature and humidity was observed and comprehensively addressed under various conditions. Areas of abnormally high or low temperature and humidity as well as major temperature and humidity gradients were recognized and thoroughly assessed based on the complete cell domain.

Results from this investigation showed the high dependence of the temperature and RH distributions on the stack flow distribution. Insufficient air plenum distance between fan and stack was determined to be a potential source of non-uniform flow distribution, resulting in more severe temperature gradients and increased drying of the MEA. In addition to the flow distribution, the air flow rate was shown to have a major effect on the cell-level hygrothermal characteristics. It was observed that by increasing the air flow rate, the maximum temperature and temperature gradients in the cell decreased. It was anticipated that at higher flow rates, due to higher convective mass transfer coefficient and higher water vapor removal rate, the overall RH in the MEA would decrease. In contrast, however, it was determined that the reduction in

temperature caused by the higher flow rates is a more influential factor, which leads to improved humidification as opposed to drying.

The thermal properties of the bipolar plate were also shown to play an important role in the hygrothermal stack behavior. The effect of the in-plane thermal conductivity was considerable on both temperature and RH variations along the channel direction and lateral direction. By increasing the in-plane thermal conductivity, the maximum temperature difference in the bipolar plate was considerably reduced, which resulted in more uniform temperature and RH distributions. Unfortunately, however, high thermal conductivities also lead to significant drying at the inlet, where the incoming air rapidly absorbs both heat and moisture from the MEA due to the heat spreading effect of the plate. In this context, high rates of in-plane heat transfer towards the inlet can have detrimental effect on the membrane hydration in this region.

Furthermore, the rate of convective heat transfer from the edges of the stack was found to affect the lateral distributions of temperature and humidity within each cell. High rates of edge heat transfer resulted in increased lateral gradients in both temperature and RH, while the maximum temperature (hot spot) at the center of the stack remained unchanged for the stack dimensions considered in this work.

In summary, based on the obtained results the following recommendations can be made for improved hygrothermal management of an air-cooled open cathode PEMFC stack:

- The fan should be positioned at an appropriate distance from the stack to avoid non-uniform distribution of air flow in the cathode channels.
- The air flow rate is a controlling parameter on the temperature and RH distributions in the stack. Increasing the flow rate results in reduced temperature and increased RH; both of which are favorable for stack operation at high current densities.
- Plate materials with high thermal conductivity may be desirable in general, but will not resolve the hygrothermal issues of open cathode stacks unless provisions are made for increasing the humidity, e.g., by increasing the flow rate. A moderate thermal conductivity is therefore recommended to achieve hygrothermal balance in open cathode cells.
- Edge cooling should generally be avoided for open cathode cells due to undesirable lateral temperature and humidity gradients.

## Acknowledgments

Funding for his research provided by Ballard Power Systems, Inc., Natural Sciences and Engineering Research Council of Canada, Western Economic Diversification Canada, Canada Foundation for Innovation, British Columbia Knowledge Development Fund, and Simon Fraser University is highly appreciated. We also gratefully acknowledge the in-kind contributions provided by Ballard Power Systems and the support from the following individuals: Julie Bellerive, David Harvey, and Shanna Knights.

## Nomenclature

|                   |                                                                   |
|-------------------|-------------------------------------------------------------------|
| $c_p$             | constant pressure specific heat, $\text{J kg}^{-1} \text{K}^{-1}$ |
| $D$               | diffusivity, $\text{m}^2 \text{s}^{-1}$                           |
| $E_{\text{th}}$   | thermal voltage, V                                                |
| $F$               | Faraday's constant, $96,485 \text{ C mol}^{-1}$                   |
| $J$               | volumetric current density, $\text{A m}^{-3}$                     |
| $k$               | thermal conductivity, $\text{W m}^{-1} \text{K}^{-1}$             |
| $M_i$             | $i^{\text{th}}$ species molar mass, $\text{kg mol}^{-1}$          |
| $p$               | pressure, Pa                                                      |
| $S$               | source term                                                       |
| $T$               | temperature, K                                                    |
| $\vec{V}$         | velocity vector, $\text{m s}^{-1}$                                |
| $V_{\text{cell}}$ | cell voltage, V                                                   |
| $x$               | lateral coordinate, m                                             |
| $x^*$             | half cell width, m                                                |
| $y$               | vertical coordinate, m                                            |
| $Y_i$             | $i^{\text{th}}$ species mass fraction                             |
| $z$               | channel (downstream) coordinate, m                                |
| $z^*$             | cell length, m                                                    |

### Greek symbols

|             |                                                          |
|-------------|----------------------------------------------------------|
| $\Delta H$  | low heating value of hydrogen, $240 \text{ kJ mol}^{-1}$ |
| $\chi_i$    | $i^{\text{th}}$ species mole fraction                    |
| $\mu$       | dynamic viscosity, Pa s                                  |
| $\phi_{ij}$ | weighting function obtained from Eq. (5)                 |
| $\kappa$    | gas permeability, $\text{m}^2$                           |
| $\rho$      | density, $\text{kg m}^{-3}$                              |

### Subscripts

|      |             |
|------|-------------|
| eff  | effective   |
| mass | mass        |
| mom  | momentum    |
| T    | temperature |

## REFERENCES

- [1] Wang CY. Fundamental models for fuel cell engineering. *Chem Rev* 2004;104:4727–65.
- [2] Sasmito AP, Birgersson E, Mujumdar AS. Numerical evaluation of various thermal management strategies for polymer electrolyte fuel cell stacks. *Int J Hydrogen Energy* 2011;36:12991–3007.
- [3] Alhazmi N, Ingham DB, Ismail MS, Hughes KJ, Ma L, Pourkashanian M. Effect of the anisotropic thermal conductivity of GDL on the performance of PEM fuel cells. *Int J Hydrogen Energy* 2013;38:603–11.
- [4] Ben Salah Y, Tabe Y, Chikahisa T. Two phase flow simulation in a channel of a polymer electrolyte membrane fuel cell using the lattice Boltzmann method. *J Power Sources* 2012;199:85–93.
- [5] Falcucci G, Jannelli E, Minutillo M, Ubertini S. Fluid dynamic investigation of channel design in high temperature PEM fuel cells. *J Fuel Cell Sci Tech* 2012;9:021014.
- [6] Hashemi F, Rowshanzamir S, Rezakazemi M. CFD simulation of PEM fuel cell performance: effect of straight and serpentine flow fields. *Math Comp Model* 2012;55:1540–57.
- [7] Jung S-P, Lee C-I, Chen C-C. An efficient method for numerical predictions of the performance characteristics of fuel cells. I. Model development and validation. *J Power Sources* 2012;199:179–94.

- [8] Eikerling M. Water management in cathode catalyst layers of PEM fuel cells. *J Electrochem Soc* 2006;153:E58.
- [9] Zamel N, Li X, Shen J. Numerical estimation of the effective electrical conductivity in carbon paper diffusion media. *Appl Energy* 2012;93:39–44.
- [10] Lange KJ, Sui P-C, Djilali N. Pore scale modeling of a proton exchange membrane fuel cell catalyst layer: effects of water vapor and temperature. *J Power Sources* 2011;196:3195–203.
- [11] Ramos-Alvarado B, Hernandez-Guerrero A, Elizalde-Blancas F, Ellis MW. Constructal flow distributor as a bipolar plate for proton exchange membrane fuel cells. *Int J Hydrogen Energy* 2011;36:12965–76.
- [12] Springer TE, Zawodzinski TA, Gottesfeld S. Polymer electrolyte fuel cell model. *J Electrochem Soc* 1991;138:2334–42.
- [13] Kermani MJ, Stockie JM. The effect of slip velocity on saturation for multiphase condensing mixtures in a PEM fuel cell. *Int J Hydrogen Energy* 2011;36:13235–40.
- [14] Shahsavari S, Desouza A, Bahrami M, Kjeang E. Thermal analysis of air-cooled PEM fuel cells. *Int J Hydrogen Energy* 2012;37:18261–71.
- [15] Ju H, Meng H, Wang C-Y. A single-phase, non-isothermal model for PEM fuel cells. *Int J Heat Mass Transf* 2005;48:1303–15.
- [16] Bapat CJ, Thynell ST. Anisotropic heat conduction effects in proton-exchange membrane fuel cells. *J Heat Transf* 2007;129:1109.
- [17] Matian M, Marquis A, Brandon N. Model based design and test of cooling plates for an air-cooled polymer electrolyte fuel cell stack. *Int J Hydrogen Energy* 2011;36:6051–66.
- [18] Choi K-S, Kim H-M, Yoon HC, Forrest ME, Erickson PA. Effects of ambient temperature and relative humidity on the performance of Nexa fuel cell. *Energy Convers Manag* 2008;49:3505–11.
- [19] Sasmito AP, Birgersson E, Mujumdar AS. A novel flow reversal concept for improved thermal management in polymer electrolyte fuel cell stacks. *Int J Therm Sci* 2012;54:242–52.
- [20] Tolj I, Bezmalinovic D, Barbir F. Maintaining desired level of relative humidity throughout a fuel cell with spatially variable heat removal rates. *Int J Hydrogen Energy* 2011;36:13105–13.
- [21] Jeon DH, Kim KN, Baek SM, Nam JH. The effect of relative humidity of the cathode on the performance and the uniformity of PEM fuel cells. *Int J Hydrogen Energy* 2011;36:12499–511.
- [22] Tanuma T, Kinoshita S. Impact of Gas diffusion layers (GDLs) on water transport in PEFCs. *J Electrochem Soc* 2012;159:B150.
- [23] Murakawa H, Ueda T, Sugimoto K, Asano H, Takenaka N. Measurement of water thickness in PEM fuel cells and analysis of gas velocity distributions. *Nucl Instrum Methods Phys Res Sect A* 2011;651:290–6.
- [24] Zhang J, Tang Y, Song C, Cheng X, Zhang J, Wang H. PEM fuel cells operated at 0% relative humidity in the temperature range of 23–120 °C. *Electrochim Acta* 2007;52:5095–101.
- [25] Fuel Cell Technologies Program. US Department of Energy web site: <http://www1.eere.energy.gov/hydrogenandfuelcells/glossary.html#c> [accessed on 20.07.12].
- [26] Mench M. Fuel cell engines. Hoboken, New Jersey: John Wiley & Sons, Inc.; 2008.
- [27] Matian M, Marquis A, Brett D, Brandon N. An experimentally validated heat transfer model for thermal management design in polymer electrolyte membrane fuel cells. *Proc Inst Mech Eng Part A J Power Eng* 2010;224:1069–81.
- [28] Kergourlay G, Kouidri S, Rankin GW, Rey R. Experimental investigation of the 3D unsteady flow field downstream of axial fans. *Flow Meas Inst* 2006;17:303–14.
- [29] Pharoah JG, Burheim OS. On the temperature distribution in polymer electrolyte fuel cells. *J Power Sources* 2010;195:5235–45.
- [30] Alofi A, Srivastava GP. Thermal conductivity of graphene and graphite. *Phys Rev B* 2013;87:115421.
- [31] Wen C-Y, Lin Y-S, Lu C-H, Luo T-W. Thermal management of a proton exchange membrane fuel cell stack with pyrolytic graphite sheets and fans combined. *Int J Hydrogen Energy* 2011;36:6082–9.